Brain, Behavior, and Immunity 128 (2025) 600–611

Contents lists available at ScienceDirect

Brain Behavior and Immunity

journal homepage: www.elsevier.com/locate/ybrbi

Full-length Article

Activation of central cannabinoid type 2 receptors, but not on peripheral immune cells, is required for endocannabinoid-mediated neuroprotection in Parkinson's disease

Leyre Ayerra [a,b], Miguel Angel Abellanas [a,b], Clara Vidaurre [a,b], Leyre Basurco [a,b], Adriana Tavira [a,b], Esther Luquin [c], Pedro Clavero [d], Elisa Mengual [c], Maria Collantes [e,f], Ivan Peñuelas [e,f], Samuel Ruiz de Martin-Esteban [g], Uwe Grether [h], Cecilia J. Hillard [i], Julian Romero [g], Sandra Hervás-Stubbs [b,f], Maria S. Aymerich [a,b,f,*]

[a] Universidad de Navarra, Facultad de Ciencias, Departamento de Bioquímica y Genética, Pamplona, Spain
[b] CIMA-Universidad de Navarra, Pamplona, Spain
[c] Universidad de Navarra, Facultad de Medicina, Departamento de Patología, Anatomía y Fisiología, Pamplona, Spain
[d] Servicio de Neurología, Hospital Universitario de Navarra, Pamplona, Spain
[e] Unidad de Imagen Molecular Traslacional (UNIMTRA), Departamento de Medicina Nuclear, Clínica Universidad de Navarra, Pamplona, Spain
[f] IdiSNA, Instituto de Investigación Sanitaria de Navarra, Pamplona, Spain
[g] Instituto de Investigaciones Biosanitarias, Facultad de Ciencias Experimentales, Universidad Francisco de Vitoria, Pozuelo de Alarcón, Madrid, Spain
[h] Roche Innovation Center Basel, F. Hoffmann-La Roche Ltd., Basel, Switzerland
[i] Department of Pharmacology and Toxicology, Neuroscience Research Center, Medical College of Wisconsin, Milwaukee, WI, USA

ARTICLE INFO

Keywords:
Parkinson's disease
Neuroprotection
Endocannabinoid system
Cannabinoid receptor type 2
Microglia
$CD4^+$ T cells

ABSTRACT

Neuroinflammation is a key feature of Parkinson's disease (PD). The cannabinoid receptor type 2 (CB2R) is expressed by cells of the innate and adaptive immune systems. Inhibition of monoacylglycerol lipase (MAGL) with JZL184 increases the levels of the endocannabinoid 2-arachidonoylglycerol (2-AG), which is neuroprotective for dopaminergic neurons. The aim of this study was to determine whether the neuroprotective effect of MAGL inhibition is mediated by CB2R activation on specific immune cell populations. Experimental parkinsonism was induced by chronic administration of MPTP and probenecid. A specific increase in $CD4^+$ T cell infiltration was detected in the midbrain of parkinsonian mice and was reduced by administration of JZL184. JZL184 had no effect in CB2R KO mice, suggesting that CB2R is required for neuroprotection. In the brain, CB2R expression was restricted to myeloid cells and lymphocytes, and increased in microglia under parkinsonian conditions. Administration of a central CB2R agonist, JWH133, exerted a beneficial effect similar to that of JZL184, whereas the peripheral agonist RO304 lacked neuroprotective activity. These results were confirmed using chimeric mice. *In silico* analysis, showed that transcripts related to 2-AG biosynthesis are downregulated in the midbrain microglia from PD patients. Our results show that activation of CB2R in the brain prevents nigrostriatal degeneration, $CD4^+$ T cell infiltration and TNFα production in the midbrain of parkinsonian mice. The reduced 2-AG signaling in microglia from PD patients suggests that activation of microglial CB2R may be an interesting strategy for the treatment of PD.

Abbreviations: 2-AG, 2-arachidonyl glycerol; AEA, Anandamide; BBB, Blood brain barrier; CB, Cytometry buffer; CB2R, Cannabinoid type 2 receptor; Chi-CB2R KO, Chimeric mice transplanted with CB2R KO HSCs; Chi-WT, Chimeric mice transplanted with WT HSCs; CI, Confidence intervals; Ctrl, Control; DAT, Dopamine transporter; ECS, Endocannabinoid system; EGFP, Enhanced green fluorescent protein; FBS, Fetal bovine serum; HSCs, Hematopoietic stem cells; i.p, Intraperitoneal; IFN, Interferon; IL, Interleukin; IPD, Idiopathic Parkinson's disease; LPS, lipopolysaccharide; MAGL, Monoacylglycerol lipase; MPTP, 1-methyl-4-phenyl-1,2,3,6-tetrahydropyridine; MPTPp, MPTP + probenecid; PBS, Phosphate-buffered saline; PD, Parkinson's disease; Prob, Probenecid; RBC, Red blood cell; RT, Room temperature; SNpc, Substantia nigra pars compacta; snRNA-seq, Single nuclei RNA sequencing; SPECT, Single photon emission computed tomography; SUV, Standardized uptake value; TH, Tyrosine hydroxylase; TNFα, Tumor necrosis factor alpha; Veh, Vehicle; WT, Wild-type.

* Corresponding author at: Cima-Universidad de Navarra, Av. Pío XII 55, 31008 Pamplona, Spain.
E-mail address: maymerich@unav.es (M.S. Aymerich).

https://doi.org/10.1016/j.bbi.2025.04.037
Received 16 December 2024; Received in revised form 3 April 2025; Accepted 28 April 2025
Available online 2 May 2025

1. Introduction

The versatility of the endocannabinoid system (ECS) places it in a key position to control the effects of neurodegeneration. Endocannabinoids are produced by both immune and neural cells (Freund et al., 2003; Salzet et al., 2000). The central location of the various elements, receptors and endocannabinoid synthesizing/degrading enzymes in the brain, allows the modulation of crucial processes such as neuroinflammation for the correct balance between neuron survival and degeneration (Aymerich et al., 2018). The immunomodulatory properties of the non-psychoactive cannabinoid type 2 receptor (CB2R) have long been known. CB2R was first described as a receptor that was not expressed in the brain, but was particularly abundant in immune cells and tissues (Munro et al., 1993; Galiègue et al., 1995). Subsequent studies showed a low expression of CB2R in microglia at steady-state conditions and in some neurons (Núñez et al., 2004; Brusco et al., 2008), which was increased in microglia under pathological conditions (Benito et al., 2003; Benito et al., 2007; Gómez-Gálvez et al., 2016). Interestingly, CB2R is expressed on cells that constitute the innate and adaptive arms of the immune system and are involved in the pathophysiology of neurodegenerative diseases.

Parkinson's disease (PD) is an age-related neurodegenerative disorder characterized by the loss of the dopaminergic nigrostriatal pathway. Neuroinflammation, a key feature of PD, has been placed at the intersection of the major risk factors, age, genetic background and environment (Tansey et al., 2022). The identification of several single-nucleotide polymorphisms in PD associated with immune system functions (Pierce and Coetzee, 2017; Nalls et al., 2019) and common genetic variants between PD and autoimmune diseases (Witoelar et al., 2017; Hui et al., 2018) highlight the relevance of the immune system in this neurodegenerative disease. The interaction between innate and T cells may be a critical immunological driver of disease pathogenesis in PD (Harms et al., 2023). Proinflammatory microglia with increased HLA-DR^+ levels (McGeer et al., 1988; Imamura et al., 2003) and expressing tumor necrosis factor alpha (TNFα), interleukin 1 beta (IL1β) and IL6 have been described in *postmortem* tissue from PD patients (Imamura et al., 2003; Hunot et al., 1999). Experimental models of PD show a dynamic activation of microglia and astrocytes in early stages of neurodegeneration that correlates with the immune cell infiltration into the midbrain (Harms et al., 2017; Ayerra et al., 2024). Evidence also points to the involvement of adaptive immune system in PD pathogenesis, but there is no consensus on the exact role played by these cells or the T cell subset involved in the disease (Brochard et al., 2009; Galiano-Landeira et al., 2020).

Circulating monocytes are altered in PD, with an increased ratio in proinflammatory classical monocytes accompanied by an activation of the CCR2-CCL2 axis (Grozdanov et al., 2014; Funk et al., 2013). Genes involved in immune activation have been detected in monocytes isolated at early stages of PD (Schlachetzki et al., 2018). A recent study concluded that perturbations of peripheral innate cell compartment in PD correlate with time and symptom severity, while changes are smaller in prodromal stages (Pike et al., 2024). Infiltrating lymphocytes have been described in the midbrain of PD patients (McGeer et al., 1988; Brochard et al., 2009; Galiano-Landeira et al., 2020). $CD4^+$ T cells with an altered migratory potential are observed in the peripheral blood of PD patients (Mamula et al., 2022). Data from a longitudinal study suggest that changes in the peripheral adaptive immune system in PD are associated with early or acute disease events in PD (Pike et al., 2024).

Modulation of specific elements of the ECS exerts different effects in experimental models of PD, symptomatic (Celorrio et al., 2016), neuroprotective (Fernández-Suárez et al., 2014) or accelerating (Celorrio et al., 2017) the time course of the disease. In this study we have focused on the neuroprotective effect of monoacylglycerol lipase (MAGL) inhibition with JZL184 *in vivo* (Fernández-Suárez et al., 2014). MAGL is the major hydrolyzing enzyme of the endocannabinoid 2-arachydonoyl glycerol (2-AG) in the brain (Blankman et al., 2007). One consequence of MAGL inhibition is an increase in 2-AG signaling, a potent modulator of peripheral and central immunity (Mecha et al., 2018), which could modulate the inflammatory response via CB2R (Gonsiorek et al., 2000) or reduce the availability of arachidonic acid required for prostaglandin synthesis (Nomura et al., 1979). *In vitro* studies from our group suggest that CB2Rs are involved in the neuroprotective effect of JZL184 (Aymerich et al., 2016), but it is unknown whether they are also involved *in vivo*. Here, we hypothesize that CB2R activation at specific locations, central *vs* periphery or innate *vs* adaptive immune cells, would be responsible for the neuroprotective effect of MAGL inhibition. Our results show that the neuroprotective effect of the MAGL inhibitor JZL184 is mediated by CB2R *in vivo* and we demonstrate that CB2R activation in the brain, but not in peripheral immune cells, is required for neuroprotection.

2. Material and methods

2.1. Animals

Adult male C57BL/6J (WT) mice, 2 months of age, were obtained from Envigo (Barcelona, Spain). MPTP was administered to male mice because females are more resistant to dopaminergic degeneration (Xu et al., 2006; Miller et al., 1998). CB2R KO and EGFP-CB2R mice of the same age were generated and donated by Drs. Romero and CJ Hillard (López et al., 2018). Mice were housed in cages with a maximum of 6 mice and maintained in a temperature (21 °C) and humidity-controlled room. Standard rodent pellet chow (Envigo) and water were provided ad libitum. Light was maintained on a 12 h light/dark cycle. All animal procedures were performed in accordance with the Spanish National Research Council's Guide for the Care and Use of Laboratory Animals. The experimental designs were approved by the Animal Experimentation Ethics Committee of the University of Navarra (Ref: 109–18, 109-18E3, 109-18E4).

2.2. MPTP intoxication and drug administration

To generate the experimental model, 4-month-old mice received 10 i.p. injections of MPTP (20 mg/kg in saline; MedChemExpress, Shanghai, China) plus probenecid (250 mg/kg in saline; Life Technologies, Oregon, USA) (MPTPp) to delay renal MPTP clearance. The compounds were co-administered in two consecutive injections twice weekly for 5 weeks. Control mice received probenecid (250 mg/kg) only in the same dosing regimen as MPTPp. Control and MPTPp mice were randomized into two groups that receiving the vehicle or the drug. Mice were treated with a MAGL inhibitor, JZL184 (8 mg/kg, i.p.; Cayman Chemical, Ann Arbor, MI, USA) (Fernández-Suárez et al., 2014), or with CB2R agonists, JWH133 (0.2 mg/kg, i.p.; Tocris Bioscience, Minneapolis, MN, USA) (Martín-Moreno et al., 2012; Aso et al., 2013) or RO6871304 (RO304, 10 mg/kg, i.p.; Roche Pharma, Switzerland) (Nettekoven et al., 2016). JWH133 crosses the blood brain barrier (BBB) (Martín-Moreno et al., 2012; Aso et al., 2013), whereas RO304 does not (Nettekoven et al., 2016). JZL184 and JWH133 were dissolved in saline (Braun, Barcelona, Spain) containing 15 % dimethyl sulfoxide (DMSO, Sigma-Aldrich), 5 % poly(ethylene glycol) (PEG, Sigma-Aldrich) and 5 % Tween-80 (Guinama, Valencia, Spain). RO304 was dissolved in saline containing 29.1 % DMSO and 5.3 % Cremophor® EL (Sigma-Aldrich).

2.3. Hematopoietic stem cell extraction

WT and CB2R KO donor mice were euthanized by CO_2 asphyxiation. The femur and tibia were removed and the epiphyseal ends were clipped to rinse the bone marrow from the bone cavity with cold cytometry buffer (CB): 5 mM EDTA (Thermo Fisher Scientific), 0.5 % fetal bovine serum (FBS, Gibco, Paisley), 100 U/mL penicillin G (Gibco), 100 μg/mL streptomycin (Gibco) in phosphate-buffered saline (PBS, Lonza, Basel, Switzerland), using a 23-gauge needle. Cells were filtered through a 70

μm nylon cell strainer and centrifuged at 300 g for 6 min. Pooled hematopoietic stem cells (HSCs) were lysed with red blood cell (RBC) lysis buffer for 5 min at room temperature (RT). Lysis was stopped by addition of CB, and after centrifugation, HSCs were resuspended in PBS at 50 x 10^6 cells/mL. HSCs were prepared less than 2 h earlier and kept on ice before injection.

2.4. Generation of bone marrow chimeras

Recipient WT mice (2 months) were irradiated with two fractions of 600 rads with a difference of 6 h. For bone marrow reconstitution, 5 x 10^6 HSCs from WT or CB2R KO animals were transplanted by intravenous administration 24 h after irradiation. Mice were treated with antibiotic (Kariflox, 5 mg/mL) in the drinking water for 4 weeks. Bone marrow was considered fully reconstituted 7 weeks after transplantation. MPTPp and JZL184 treatments were started after this time.

2.5. Motor behavior

Pole, bar and rotarod tests were performed to analyze the motor behavior of the mice. The pole and bar tests were performed 4 h after the last MPTP injection and the rotarod 16 h later. Behavioral tests were performed under low light conditions. In the pole test, animals were placed upright on the top of a vertical wooden pole, 50 cm high and 1 cm in diameter, covered with a bandage. Animals were pre-trained until they were able to turn their head down and to descend from the pole in less than 5 s. The mean time to turn their head down and completely descend from the pole was measured in two trials with a 15 min rest period between each trial. In the bar test, animals were placed with their forepaws on a bar parallel 4 cm above the ground. The mean time to move the forepaws to the ground was measured in three consecutive trials. In the rotarod test (LE8200, Panlab, Barcelona, Spain), animals were placed over a moving rod, which was programmed to rotate at increasing speeds from 4 rpm to 40 rpm in 5 min. Animals were pre-trained on two consecutive days until they were able to remain over the rod for at least 1 min. The average time that each mouse remained on the rod was recorded in two trials with a 30 min rest period in between.

2.6. Blood extraction

Submandibular blood samples (50 μL) were collected in EDTA microvette-coated tubes (BD Biosciences, Franklin Lakes, NJ, USA), mixed with 750 μL of RBC and incubated for 15 min at RT on a rotating shaker. Samples were centrifuged at 1200 g for 15 min at RT, cells were washed and the pellet was resuspended in 100 μL of CB for flow cytometry.

2.7. Preparation of brain cell suspensions

Adult mice were anesthetized with i.p. ketamine/xylazine and perfused transcardially with ice-cold PBS. The brain was removed and the striatum and ventral midbrain were dissected on ice. The tissue was digested with a collagenase D mixture (400 units/mL, Roche, Mannheim, Germany) or a papain mixture (2 mg/mL, Worthington, Lakewood, NJ, USA), containing the enzyme DNase-I (50 μg/mL, Sigma-Aldrich) in Dulbecco's PBS (DPBS, Lonza, Basel, Switzerland). Digestion was performed at 37 °C with rotation for 15 min with collagenase D or for 30 min with papain. The samples were cooled down and 10 μL of EDTA 500 mM (Invitrogen, Carlsbad, CA, EEUU) were added to stop the reaction. Brain tissue was mechanically dissociated with a glass Pasteur pipette, filtered through a 70 μm nylon cell and centrifuged at 300 g for 15 min at 4 °C. Samples were resuspended in 25 % Percoll (GE Healthcare, Chicago, IL, EEUU) and centrifuged at 1000 g for 10 min at RT to remove cell debris and myelin. The white layer was carefully removed and the cell pellet was resuspended in 100 μL of CB or RPMI medium (Invitrogen) for flow cytometry.

2.8. Flow cytometry

Cell pellets obtained from the brain were resuspended in 100 μL of CB and incubated with Zombie NIR dye (BioLegend, San Diego, CA, USA) for 5 min at RT to assess the percentage of cell viability (50 μL/sample; 1:2000 dilution in PBS). Zombie NIR dye was quenched with 150 μL of CB and cells were centrifuged at 2000 rpm for 1 min. Cells were labeled with a panel of fluorescent antibodies diluted in CB and the FcR blocking reagent (1:50; Miltenyi Biotec, Bergisch Gladbach, Germany) for 15 min at 4 °C: BV510 anti-CD11b (1:500, M1/70, BioLegend) or VioBlue anti-CD11b (1:100, M1/70.15.11.5, Miltenyi Biotec), BV421 anti-CD45 (1:1000, 30F11, BioLegend) or BV510 anti-CD45 (1:1000, 30F11, BioLegend), APC anti-ACSA2 (1:50, IH3-18A3, Miltenyi Biotec), BUV395 anti-CD8a (1:200, 53–6.7, BD Bioscience), BV711 anti-CD4 (1:200, GK1.5, BioLegend) and PerCP-Vio700 anti-CD3 (1:50, 145-2C11, Miltenyi Biotec). In EGFP-CB2R transgenic mice, EGFP was detected directly using a 488 nm laser. Cell pellets obtained from blood samples were incubated with Zombie NIR and labeled with the following panel of fluorescent antibodies: BV510 anti-CD11b (1:500, M1/70, BioLegend), BV421 anti-CD45 (1:1000, 30F11, BioLegend) and PerCP-Cy5.5 anti-CD3 (1:200, 145-2C11, BioLegend). After centrifugation, they were labeled with a primary antibody rabbit anti-CB2R (1:25, Cayman Chemical) in CB during 15 min at RT, washed and incubated with a secondary antibody Alexa Fluor 647 goat anti-rabbit (1:100, Invitrogen) under the same conditions. After labeling, samples were centrifuged, resuspended in CB, acquired on a CytoFLEX LX flow cytometer (Beckman Coulter, Brea, CA) and analyzed using the CytExpert 2.3 (Beckman Coulter) and FlowJo 10.0.7r2 (BD Biosciences, Franklin Lakes, NJ) software.

2.9. In vitro T cell stimulation for intracellular cytokine profiling

To assess TNFα production by lymphocytes, midbrain cell pellets were resuspended in 100 μL of RPMI supplemented with 10 % FBS, 100 U/mL penicillin G, 100 μg/mL streptomycin, 10 μg/mL gentamicin solution, 50 μM β-mercaptoethanol and 12.5 mM HEPES buffer instead of CB. A combined solution of phorbol 12-myristate 13-acetate [PMA 0.05 μg/mL (Sigma-Aldrich)/ionomycin 0.5 μg/mL (Sigma-Aldrich)] was then added to stimulate T cell cytokine production. Brefeldin-A 5 μg/mL (BioLegend) was used to block cytokine transport. After incubation at 37 °C for 4 h, samples were centrifuged at 2000 rpm for 1 min and washed with PBS. Cells were first labeled with cell surface markers for flow cytometry as described previously and incubated with a fixation/permeabilization solution (Invitrogen) for 7 min at 4 °C in the dark. Cells were then centrifuged under the same conditions and washed with PermWASH solution (Invitrogen). After further centrifugation, the cells were labeled with an intracellular panel of fluorescent antibodies diluted in PermWASH solution during 15 min at 4 °C in the dark: PE-Cy7 anti-TNFα (1:400, MP6-XT22, BioLegend). After labeling, samples were centrifuged, resuspended in CB, collected on a CytoFLEX LX flow cytometer and analyzed using the CytExpert 2.3 and FlowJo 10.0.7r2 software.

2.10. Histological techniques

Animals were anesthetized with i.p. ketamine/xylazine and perfused transcardially with Ringer's solution (145.4 mM NaCl, 3.4 mM KCl, 2.4 mM $NaHCO_3$, pH 7.4) for 5 min at a rate of 9.5 mL/min and with 4 % paraformaldehyde (PFA; Panreac, Barcelona, Spain) in 0.125 M PBS (pH 7.4) for 10 min. Brains were removed, post-fixed in 4 % PFA for 24 h and stored in 30 % sucrose/PBS until decanting. Coronal 40 μm thick sections were cut on a Leica SM2000R sliding microtome (Leica, Wetzlar, Germany). Free-floating sections were washed with PBS and endogenous peroxidase activity was inactivated for 30 min with 0.03 % H_2O_2 (Sigma-Aldrich)/methanol (Panreac). The sections were washed with PBS and incubated with blocking solution [4 % normal goat serum, 0.05

% Triton X-100 (Sigma Aldrich) and 4 % BSA (Merck, Darmstadt, Germany) in PBS] for 40 min. Rabbit anti-tyrosine hydroxylase (TH; 1:1000, Merck Millipore), guinea pig anti-Iba1 (1:1000; Synaptic Systems, Göttingen, Germany) and rabbit anti-CB2R (1:25, Cayman Chemical) were diluted in blocking solution and incubated overnight at RT. For immunohistochemistry, sections were then incubated with a biotinylated goat anti-rabbit secondary antibody (1:500, Jackson ImmunoResearch, Ely) in blocking solution for 2 h at RT, with peroxidase-conjugated avidin (1:5000, Sigma-Aldrich) for 90 min at RT and, after washing with PBS, with 0.05 % diaminobenzidine (Sigma-Aldrich), 0.03 % H_2O_2 and Trizma-HCl buffer (pH 7.6). For immunofluorescence, antibody binding was detected by incubating sections with the secondary antibodies diluted in blocking solution for 2 h at RT and protected from light: Alexa Fluor 594 goat anti-guinea pig (1:500; Invitrogen) and Alexa Fluor 647 goat anti-rabbit (1:100; Invitrogen). Finally, the tissue was stained with DAPI (1:50,000; Sigma-Aldrich). Tissues were mounted on glass slides in a 0.2 % solution of gelatin in 0.05 M Tris-HCl buffer (pH 7.6) (Sigma-Aldrich), dried overnight and dehydrated in toluene (Panreac) for 12 min. Finally, the slides were coverslipped with DPX (BDH Chemicals, Poole).

2.11. Image analysis

Images were captured on an Aperio C52 digital pathology slide scanner (Leica) at a 20 × magnification. Optical density values of TH immunoreactivity were obtained from 6 striatal sections per animal taken at equal intervals (360 μm) by using ImageJ (National Institutes of Health, MD). For TH density analysis, a random region of the cortex was used as a blank and its value was subtracted from the intensity of both striatal hemispheres. TH^+ neurons in the SNpc were counted in 6–7 coronal sections per animal taken at equal intervals (160 μm) covering the entire nucleus. Unbiased design-based stereology was performed using a Bx61 microscope (Olympus, Hicksville, NY) equipped with a DP71 camera (Olympus), a stage connected to a xyz stepper (H101BX, PRIOR) and Stereo Investigator software (version 2021.1.1; MBF Bioscience, Williston, VT). The reference volume (Vr) was calculated from images obtained with the 2 × objective using a point count array according to Cavalieri principles (Gundersen and Jensen, 1987). Measurement of the cross-sectional area of the nucleus and estimation of the Vr were determined using the following equation:

$$Vr = T\frac{a}{p}\sum Pi$$

where T is the section thickness, a/p is the area of each point and Pi corresponds to the number of points falling within the SNpc. SNpc masks were outlined with the 10 × objective to estimate the area. TH^+ neurons were counted at 100 × magnification under oil immersion, using randomized meander sampling and the optical dissector methods. To count a minimum of 100–150 cells/animal a sampling frame of 4900 μm^2 and sampling steps of 181 μm × 181 μm (dx, dy) were used for control mice and 140 μm × 140 μm (dx, dy) were used for MPTPp mice. The total number of TH^+ neurons (N) was calculated using the following formula:

$$N = \sum Q^{-}\frac{t}{h}\frac{1}{asf}\frac{1}{ssf}$$

where ΣQ^- is the number TH^+ cells counted, t is the mean of the section thickness, h is the height of the optical dissector, asf is the area sampling fraction, and ssf is the section sampling fraction. The density of TH^+ neurons (D) was determined using the following formula: D = N/Vr. Gunderson's coefficients of error were < 0.1 for all stereological quantifications.

Confocal images of the double staining Iba1/CB2R were acquired on a LSM800 confocal microscope (Zeiss, Jena, Germany) using the 63x oil objective. A projection stack with the same number of images per slice was generated. We generated an ImageJ plugin to calculate colocalization volume (μm^3) defined as particles with size larger than 20 pixels to extract the volume of CB2R inside $Iba1^+$ cells. 3D reconstructions of Iba1/CB2R staining were generated using Imaris software (Bitplane) and ImageJ.

2.12. Analysis of processed snRNA-seq data from Parkinson's disease patients

Single nuclei RNA sequencing (snRNAseq) data from the midbrain of idiopathic PD (IPD) patients (Smajic et al., 2022) were analyzed to determine the transcriptome profile of the ECS in glial cells. Differentially expressed genes in the IPD midbrain microglia (*CD74*) and astrocytes (*AQP4*) with $q < 0.05$ were downloaded from Smajić et al., 2022 (Smajic et al., 2022). Transcripts related to synthesis, degradation and intracellular signaling of the endocannabinoids were examined in the gene set lists and upregulated (estimate > 0) and downregulated (estimate < 0) genes were graphed.

2.13. Statistical analysis

GraphPad Prism version 8.0 was used to generate the graphs for statistical analysis. All data are presented as means with 95 % confidence intervals (CI). The normal distribution of the data was analyzed using the Shapiro-Wilk test. To compare two experimental groups, student's *t*-test (two-tailed) for equal variances was used for data following a normal distribution, and Welch's correction was applied when variances were significantly different. The Mann-Whitney *U* test was used to evaluate data not following a normal distribution. For the analysis of one variable, we used one-way ANOVA and Bonferroni's multiple comparison test for data following a normal distribution or Kruskal-Wallis and by Dunn's multiple comparison test for data not following a normal distribution. Two-way ANOVA followed by Bonferroni's post hoc test was used to analyze two variables. p-values < 0.05 were considered as statistically significant.

3. Results

3.1. $CD4^+$ T cell infiltration in the ventral midbrain correlates with the extent of neuronal degeneration in the MPTPp mouse model

MAGL inhibition with JZL184 increases brain 2-AG levels and protects the nigrostriatal pathway from MPTP-induced dopaminergic degeneration (Suppl. Fig. 1) (Fernández-Suárez et al., 2014). Administration of the radioligand [^{123}I]-Ioflupane to visualize the presynaptic dopamine transporter (DAT) showed that JZL184-treated animals had similar radioligand binding in the basal ganglia as control mice (Suppl. Fig. 2). These results demonstrate that JZL184 preserves dopaminergic terminals in the MPTPp mouse model, which may account for the improvement in motor behavior. In this context, we asked whether modulation of the immune system might be involved in the neuroprotective effect of JZL184. We prepared cell suspensions from the striatum and the ventral midbrain to analyze immune cells by flow cytometry. The gating strategy used to select immune cell subpopulations is shown in Fig. 1A. Myeloid cells were identified by the expression of CD11b and CD45, the $CD11b^+CD45^{low}$ gate was assigned to resident microglia and the $CD11b^+CD45^{high}$ gate to myeloid infiltrating cells and resident activated microglia. $CD4^+$ and $CD8^+$ T cells were selected from the $CD11b^-CD45^{high}$ population (Fig. 1A). A specific increase in $CD4^+$ T cell infiltration was observed in the ventral midbrain of MPTPp mice ($F_{1,20} = 6.3$, $p_{int} = 0.02$), but not in JZL184-treated animals (Fig. 1B). No differences were found in striatal $CD4^+$ T cell infiltration (Fig. 1B), $CD8^+$ T cells (Fig. 1C), $CD11b^+CD45^{low}$ (Fig. 1D) or $CD11b^+CD45^{high}$ (Fig. 1E). These results suggest an association between $CD4^+$ T cell infiltration in the ventral midbrain and dopaminergic neuronal cell death.

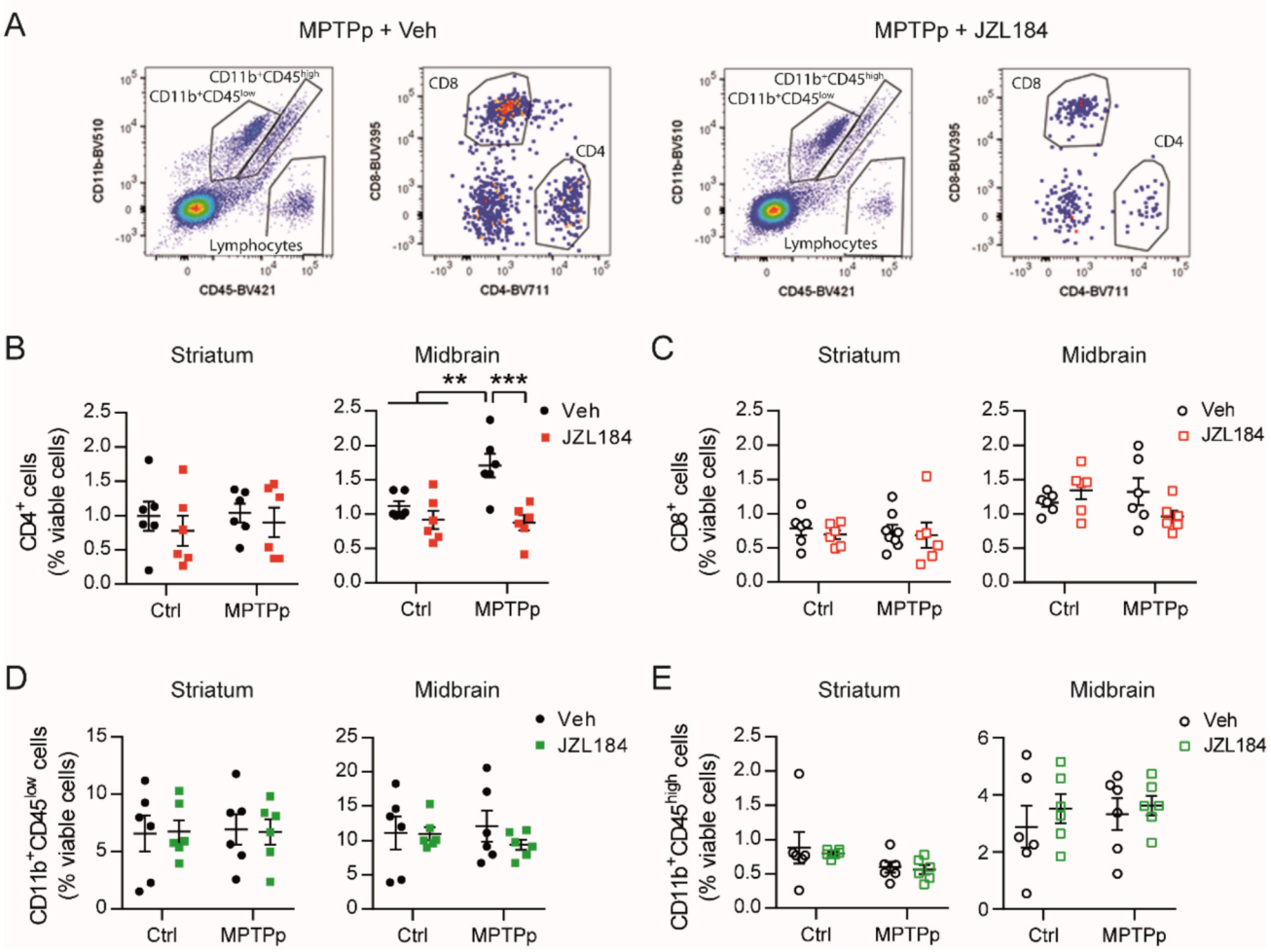

Fig. 1. Immune cell infiltration into the brain parenchyma in MPTPp mice treated with JZL184. Experimental parkinsonism was induced with 10 doses of MPTP (20 mg/kg) and probenecid (250 mg/kg) (MPTPp) administered concurrently for 5 weeks. Control animals received probenecid on the same days. JZL184 (8 mg/kg) was administered 5 days/week during the 5 weeks starting 6 h after the first MPTP injection. Mice were sacrificed 48 h after the last MPTPp injection to prepare cell suspensions from the striatum and the ventral midbrain for flow cytometry. (A) Dot plot showing the gating strategy for myeloid cells, microglia ($CD11b^{+}CD45^{low}$) and monocytes/macrophages or activated microglia ($CD11b^{+}CD45^{+high}$), and $CD4^{+}$ and $CD8^{+}$ T cells within the $CD11b^{-}CD45^{high}$ gate in the ventral midbrain. Fraction of (B) $CD4^{+}$ and (C) $CD8^{+}$ lymphocytes, (D) $CD11b^{+}CD45^{low}$ and (E) $CD11b^{+}CD45^{+high}$ myeloid cells among viable cells in the striatum and in the ventral midbrain. Data represent the mean ± 95 % CI from 6 animals/group. Statistical analysis: Two-way ANOVA followed by Bonferroni's test for multiple comparisons test, $^{**}p < 0.01$, $^{***}p < 0.001$.

3.2. CB2R in immune cells is required for the neuroprotective effect of JZL184

We next asked whether immune cells are directly involved in the neuroprotective effect of JZL184 or are indirectly affected by the improvement in neuronal survival. First, we examined the cellular selectivity of CB2R expression by flow cytometry using transgenic EGFP-CB2R mice (López et al., 2018) (Fig. 2A). The CB2R expression pattern was similar in the striatum and in the ventral midbrain, with $CD11b^{+}CD45^{high}$ myeloid cells exhibiting the highest levels of CB2R followed by $CD11b^{+}CD45^{low}$ and $CD3^{+}$ cells. No EGFP signal was observed in astrocytes ($ACSA2^{+}$) and in the negative fraction (Fig. 2A). Intoxication with MPTPp differentially modulated CB2R levels in the striatum and in the ventral midbrain (Fig. 2B). In the midbrain, CB2R expression was increased in $CD11b^{+}CD45^{low}$ cells and decreased in $CD11b^{+}CD45^{high}$ cells, whereas a trend was observed in striatal $CD3^{+}$ cells (Fig. 2B). Increase of microglial CB2R expression was confirmed by flow cytometry and double staining of Iba1 and CB2R 35 days after the first MPTP injection (Fig. 2C and 2D). MPTPp intoxication induced a significant increase in CB2R expression in EGFP-CB2R mice compared to control animals (Fig. 2C). Colocalization volume of Iba1 and CB2R increased in WT MPTPp mice compared to the control group (Fig. 2D). Data were normalized with the mean value of the signal in MPTPp CB2R KO mice to guarantee the specificity of the analysis (Fig. 2C and 2D). At 35 days, where the CB2R expression reaches its highest value in microglia from MPTPp parkinsonian mice (Fig. 2B,2C and 2D), we have analyzed the expression of inflammatory transcripts in this glial cell population. We have prepared a heatmap which indicates a proinflammatory polarization of microglial phenotype in the midbrain at this temporal point (Suppl. Fig. 3), as we have found an increased expression of genes such as *CD93*, *CD44*, *Tnfsf9*, *Ifitm6* and *Il11ra1*. Moreover, we found a decrease of classical antiinflammatory microglial genes such as *Trem2*, *Aif1* or *Cx3cr1*. Therefore, the increase in CB2R expression correlates with the appearance of a proinflammatory response in microglia as it has been described in the literature (Benito et al., 2003; 2007; Gómez-Gálvez and Palomo-Garo, 2016; Mecha et al., 2015; Reusch et al., 2022).

To determine whether the beneficial effect of JZL184 was mediated by CB2R, constitutive CB2R KO mice (López et al., 2018) were intoxicated with MPTPp and treated with the drug for 5 weeks. Analysis of motor behavior in the pole, rotarod and bar tests showed that JZL184 did not improve motor behavior in treated parkinsonian mice (Fig. 3A).

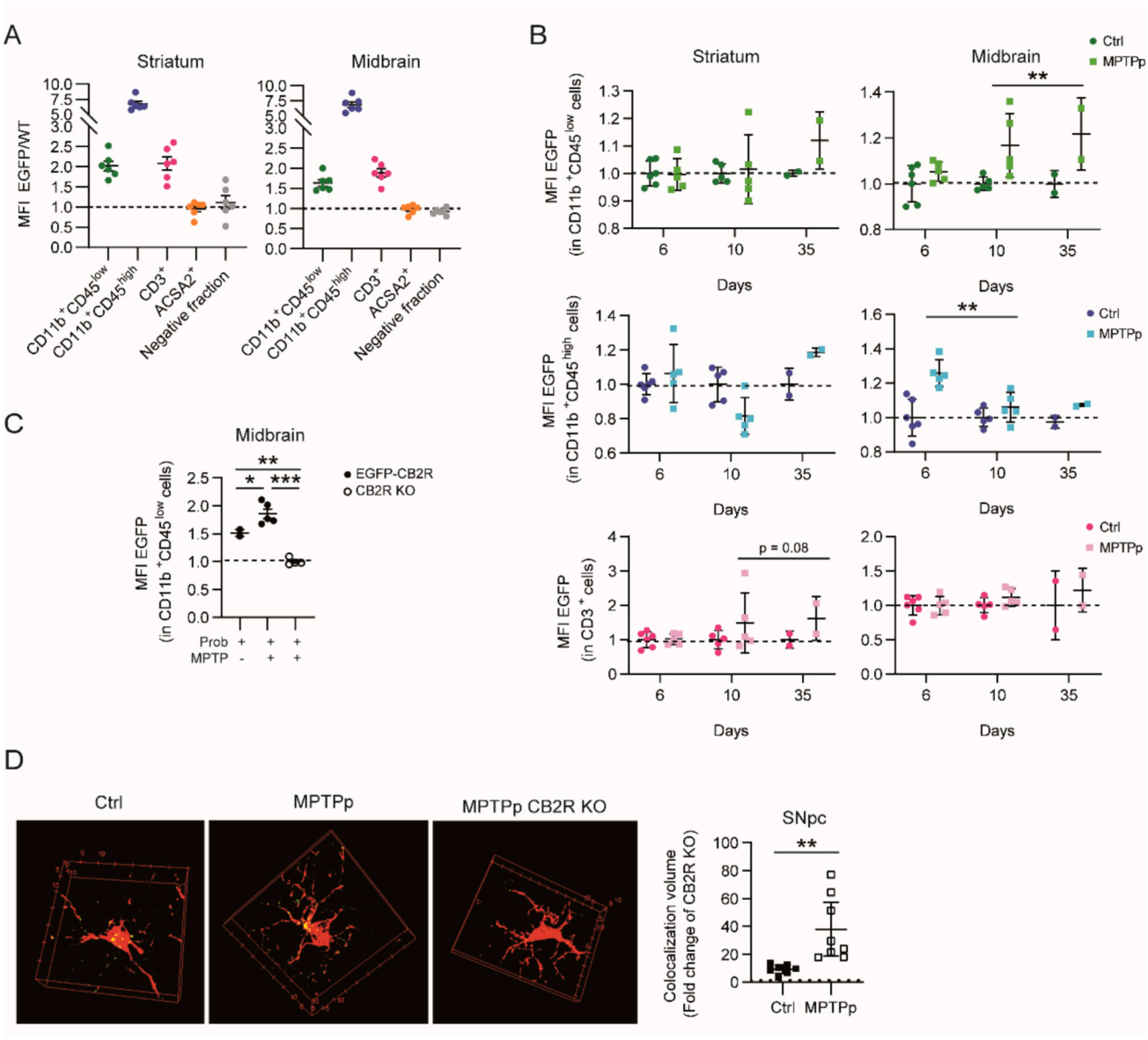

Fig. 2. Cell type specific CB2R expression in the striatum and ventral midbrain and changes in CB2R expression along MPTPp intoxication. Transgenic EGFP-CB2R mice were used to detect EGFP in different cell subsets by flow cytometry. (A) CB2R expression under physiological conditions in $CD11b^{+}CD45^{low}$, $CD11b^{+}CD45^{high}$, $CD3^{+}$, $ACSA2^{+}$ cells and the negative fraction obtained from the striatum and ventral midbrain. (B) Evolution of CB2R expression in $CD11b^{+}CD45^{low}$, $CD11b^{+}CD45^{high}$ and $CD3^{+}$ cells in the striatum and ventral midbrain during MPTPp-induced degeneration. (C) Fold change of CB2R expression in control and MPTPp EGFP-CB2R mice 35 days after the first MPTP injection. The mean value of the signal in MPTPp CB2R KO mice was used as negative control. (D) WT and transgenic CB2R KO mice were used to analyze CB2R expression in $Iba1^{+}$ cells 35 days after the first MPTP injection. Representative 3D reconstructions of Iba1/CB2R double immunofluorescence in the SNpc of control and MPTPp WT mice and in MPTPp CB2R KO mice as negative control. Fold change of Iba1-CB2R colocalization volume. Data represent the mean ± 95 % CI from 2 to 8 animals/group. Statistical analysis: (B) Two-way ANOVA. (C) One-way ANOVA followed by Bonferroni's multiple comparison test. (D) *t*-test with Welch correction, $*p < 0.05$, $**p < 0.01$, $***p < 0.001$. Magnification bars: (D) 5 and 10 μm.

Under these conditions $CD4^{+}$ T cells infiltrating the ventral midbrain remained significantly elevated (Fig. 3B). These results suggest that CB2R is required for the action of JZL184.

To validate the neuroprotective effect of CB2R activation, MPTPp mice were treated with the CB2R agonist JWH133, which is able to cross the BBB (0.2 mg/kg) (Martín-Moreno et al., 2012; Aso et al., 2013; Soethoudt et al., 2017). Motor behavior (Fig. 4A) was significantly improved in the pole ($F_{1,20} = 11$, $p_{int} = 0.003$), rotarod ($F_{1,20} = 29.5$, $p_{int} < 0.0001$) and bar tests ($F_{1,20} = 10.8$, $p_{int} = 0.004$). Immunohistochemical analysis revealed a specific increase in TH immunostaining in the striatum (Fig. 4B, $F1_{,20} = 22$, $p_{int} = 0.0001$) and a higher number of TH^{+} neurons in the SNpc compared to untreated animals (Fig. 4C, $F1_{,20} = 8.6$, $p_{int} = 0.008$). These results demonstrate that CB2R activation is neuroprotective in the MPTPp mouse model of PD.

3.3. Activation of CB2R in microglia, but not in lymphocytes, protects the nigrostriatal pathway

We next asked whether activation of CB2R present in the brain or in peripheral immune cells is required for neuroprotection. To this end, MPTPp mice were treated daily for 5 weeks with RO304 (10 mg/kg), a CB2R agonist that does not cross the BBB (Nettekoven et al., 2016; Porter et al., 2019). RO304 did not improve motor behavior in the pole, rotarod and bar tests (Fig. 5A). Histological assessment of the nigrostriatal pathway showed a lack of protection of striatal TH^{+} terminals (Fig. 5B) and dopaminergic neurons in the SNpc (Fig. 5C). We then

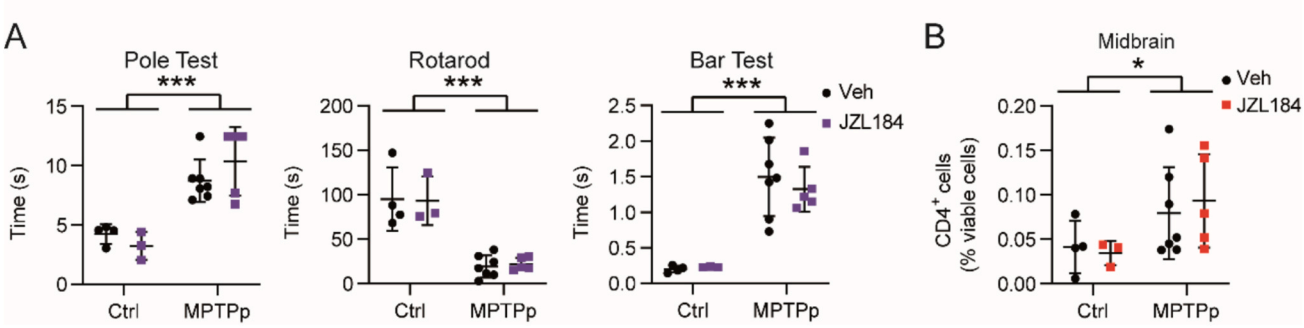

Fig. 3. Effect of JZL184 treatment in CB2R KO mice intoxicated with MPTPp. Constitutive CB2R KO mice were intoxicated with MPTPp and treated with JZL184 during 5 weeks. (A) Analysis of motor behavior in the pole, rotarod and bar tests. (B) Upon sacrifice 48 h after the last MPTPp dose, the ventral midbrain was processed for flow cytometry to analyze $CD4^+$ T cell infiltration. Data represent the mean ± 95 % CI from 3 to 7 animals/group. Statistical analysis: Two-way ANOVA, $*p < 0.05$, $***p < 0.001$.

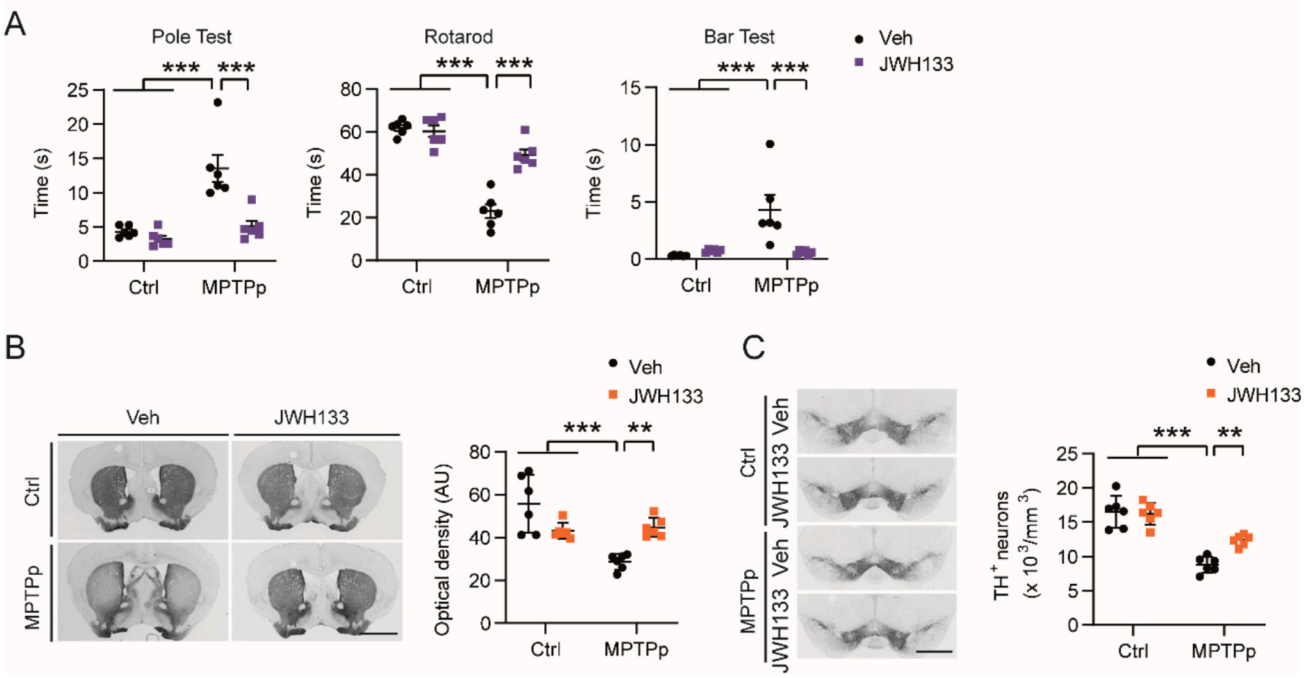

Fig. 4. Neuroprotective effect of JWH133 administration in the MPTPp mouse model. Experimental parkinsonism was induced with the administration of MPTPp for 5 weeks. JWH133 (0.2 mg/kg) was administered i.p. daily starting 6 h after the first MPTP injection until the time of sacrifice. (A) Motor behavior was assessed using the pole, rotarod and bar tests. (B) Representative photomicrographs showing TH immunoreactivity in the striatum and the optical density analysis of the TH signal. (C) Representative images showing TH^+ dopaminergic neurons in the SNpc and the unbiased stereological quantification of the number of TH^+ neurons. Data represent the mean ± 95 % CI from 6 animals/group. Statistical analysis: Two-way ANOVA followed by Bonferroni's for multiple comparisons, $**p < 0.01$, $***p < 0.001$. Magnification bars: (B) 2 mm, (C) 1 mm.

compared the effect of JZL184, JWH133 and RO304 on the immune response. The infiltration of $CD4^+$ T cells in the striatum and in the midbrain was maintained in MPTPp mice treated with RO304 and vehicle, and was significantly reduced by JWH133 treatment (Fig. 6A), while no effect was observed for $CD8^+$ T cells (Fig. 6B). Myeloid $CD11b^+CD45^{low}$ cells were significantly increased by both treatments (Fig. 6C), and $CD11b^+CD45^{high}$ cells were increased by RO304 (Fig. 6D) in the ventral midbrain. These results demonstrate that administration of RO304 is unable to reproduce the neuroprotective effect of JWH133, suggesting that activation of CB2R in the brain parenchyma is necessary for neuroprotection. JZL184 and JWH133 had a similar effect on immune cells in the midbrain, but differed in the striatum, where JWH133 reduced $CD4^+$ T cell infiltration in this region but JZL184 did not. The different mechanism of action of the two drugs may be responsible for this effect. Since JZL184 increases the levels of 2-AG, the endogenous ligand for the cannabinoid receptors CB1R and CB2R, it may exert a broader range of effects beyond CB2R activation. In contrast, JWH133 is a highly specific CB2R agonist, in which case its effect would be limited to cells expressing these receptors. Independently of their differential effect on striatal T cell infiltration, both neuroprotectants reduced MPTP-induced TNFα production in $CD4^+$ and in $CD8^+$ T cells in the ventral midbrain (Fig. 6E). No significant differences in TNFα-positive lymphocytes in this region were observed between MPTPp mice treated with vehicle or RO304 (Fig. 6E).

To determine which CB2R-expressing cells in the brain parenchyma are necessary for neuroprotection, we generated bone marrow chimeric mice. Irradiated WT mice were transplanted with HSCs from WT (Chi-WT) or CB2R KO (Chi-CB2R KO) donor mice (Fig. 7A). A significant decrease in CB2R expression was observed in $CD3^+$ and $CD11b^+CD45^{high}$ cells in the periphery 7 weeks after transplantation with CB2R KO HSCs (Fig. 7B). MPTPp-intoxicated chimeric mice treated with JZL184 performed similarly to control mice in the pole, rotarod and

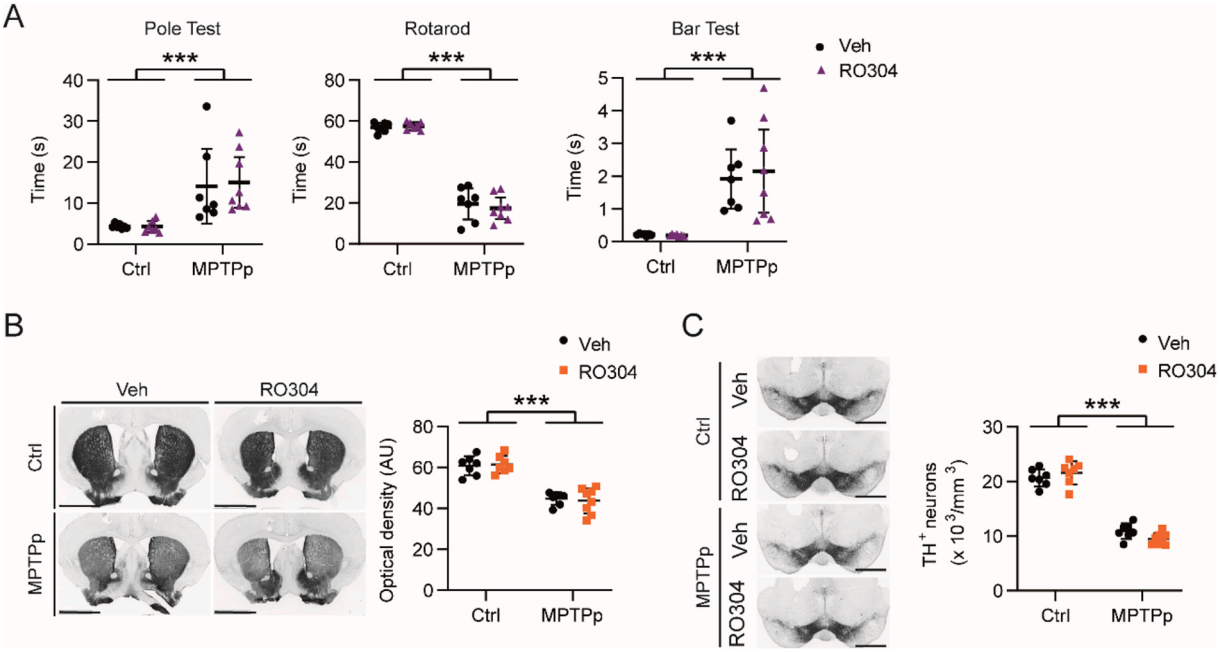

Fig. 5. Lack of effect of RO304 treatment in the MPTTp mouse model. Experimental parkinsonism was induced with the administration of MPTTp for 5 weeks. RO304 (10 mg/kg) was administered i.p. daily starting 6 h after the first MPTP injection until the time of sacrifice. (A) Motor behavior was assessed in the pole, rotarod and bar tests. (B) Representative photomicrographs showing TH immunoreactivity in the striatum and the optical density analysis of the TH signal. (C) Representative images showing TH^+ dopaminergic neurons in the SNpc and unbiased stereological quantification of the number of TH^+ neurons. Data represent the mean ± 95 % CI of 7–8 animals per group. Statistical analysis: Two-way ANOVA followed by Bonferroni's for multiple comparisons, $^{***}p < 0.001$. Magnification bars: (B) 2 mm, (C) 1 mm.

bar tests and significantly better than untreated MPTTp mice (Fig. 7C). TH immunostaining in the striatum (Fig. 7D) and stereological quantification of TH^+ neurons in the SNpc (Fig. 7E) showed that the neuroprotective effect was maintained in the absence of peripheral CB2R. Since microglia are radio-resistant and thus cannot be replaced by HSCs transplantation (Mildner et al., 2007), Chi-WT and Chi-CB2R KO mice showed similar levels of CB2R expression in $Iba1^+$ cells independent of transplantation (Fig. 7F). These results suggest that CB2R activation in the brain, probably in microglial cells, but not in infiltrating peripheral immune cells is necessary for neuroprotection. CB2R agonists do not appear to have a direct effect on T cells, but the indirect reduction of TNFα production may contribute to their neuroprotective effect.

3.4. The 2-AG biosynthesis is downregulated in the midbrain microglia of PD patients

To determine the transcriptomic profile of the ECS in PD, we took advantage of single nucleus RNA sequencing (snRNA-seq) data obtained from the midbrain of 6 idiopathic PD patients with severe neuronal loss and 5 age-matched controls (Smajic et al., 2022). Differentially expressed transcripts associated with the ECS (Fig. 8A) were searched for in glial cell populations. Differentially expressed genes in glia were more related to 2-AG metabolism than to anandamide (AEA) (Fig. 8B). In microglia (*CD74*), a decrease in 2-AG biosynthesis-related transcripts (*DAGLB, PLCB2, PDIA3*) and an increase in the degradation enzyme *ABHD3* suggest a decrease in 2-AG production. In astrocytes (*AQP4*), the increase in both, biosynthesis (*PLCH1, PLCG2, PLCB4, PDIA3*) and degradation related transcripts, such as *MGLL*, indicate an accelerated turnover of this molecule. Transcripts related CB1R or CB2R expression were not differentially expressed in human PD midbrain cells. This may be related to the advanced stage of the neuronal loss in the subjects analyzed (Lewy body Braak stage 5/6). Considering the decreased 2-AG production and the resulting insufficient CB2R activation in microglia from PD patients to resolve the insult and promote an antiinflammatory environment in the brain parenchyma, our results suggest that pharmacological CB2R activation may be an interesting therapy for PD.

4. Discussion

In the present study, we have investigated the mechanisms underlying the neuroprotective effect of MAGL inhibition with JZL184. We identified a specific increase in $CD4^+$ T cell infiltration in the ventral midbrain of MPTTp mice, which was not observed in JZL184-treated animals. Experiments with CB2R KO mice suggest that the mechanism of action of JZL184 is mediated by CB2R. Using selective CB2R agonists and chimeric mice we have shown that CB2R activation in the brain, probably in microglia, but not in peripheral immune cells, is required for neuroprotection in the chronic experimental model of PD. The decreased expression of 2-AG synthesizing enzymes in human microglia suggests a reduced production of this endogenous CB2R ligand in PD and supports the potential beneficial effect of CB2R ligands that reach the CNS for the treatment of this neurodegenerative disease.

Inflammation is a central feature of PD, and it is therefore necessary to understand the interactions between the immune system and neuronal survival in order to develop effective immunomodulatory therapies. For this study, we chose the MPTTp mouse model because, as we have recently described, it is the model that best recapitulates the glial activation described in the human midbrain (Ayerra et al., 2024). The activation state of glial cells in experimental models of PD based on α-synuclein overexpression or MPTTp intoxication correlates with $CD4^+$ T cell infiltration in the midbrain (Ayerra et al., 2024; Harms et al., 2013; Basurco et al., 2023). Infiltrated $CD4^+$ T cells have been described in the midbrain of PD patients (McGeer et al., 1988; Brochard et al., 2009). Dynamic changes in $CD4^+$ lymphocyte numbers and activation are associated with PD progression, and an increase in $CD4^+$ naïve T cells after clinical diagnosis of PD suggests that neurodegeneration may contribute to $CD4^+$ T cell recruitment to the CNS (Pike et al., 2024). The neuroprotection provided by JZL184 and JWH133 correlates with reduced $CD4^+$ T cell infiltration into the midbrain, an effect that is not observed in CB2R KO mice. This could be due to the inhibition of

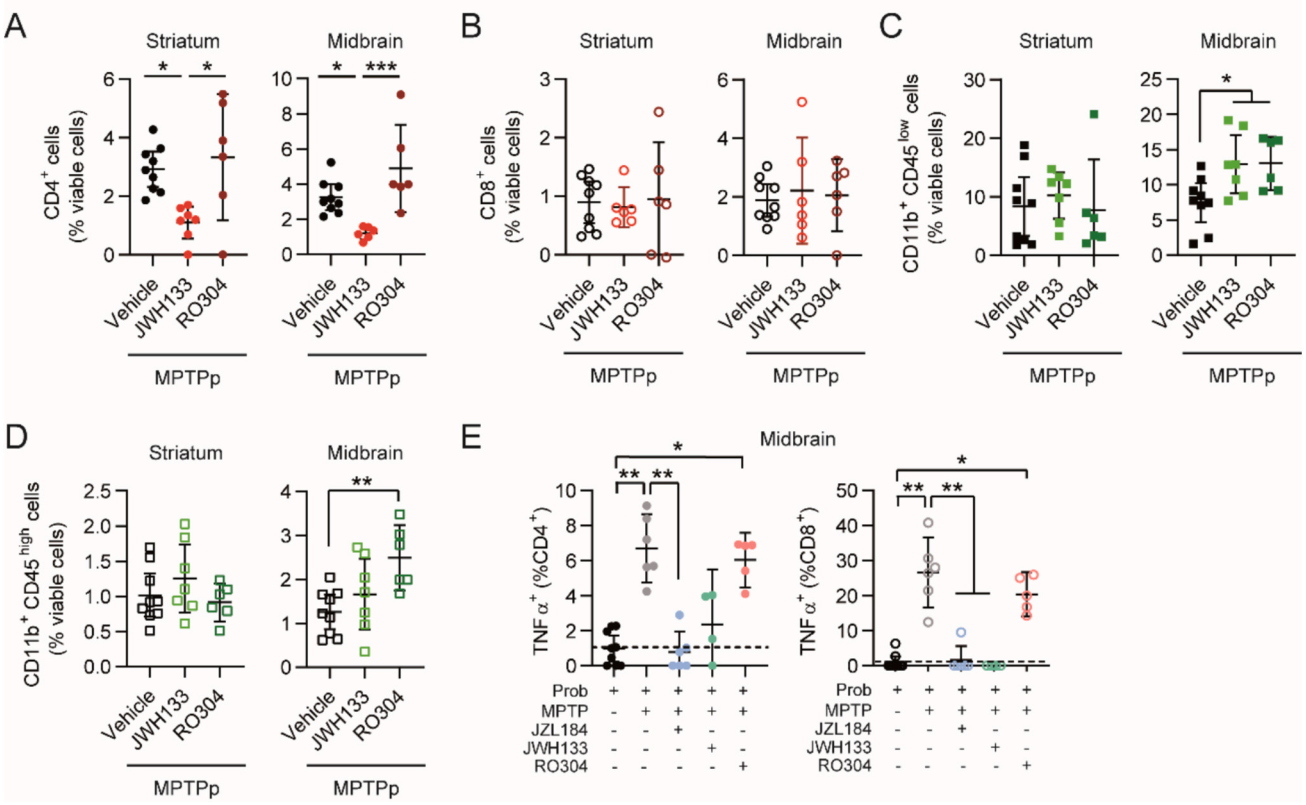

Fig. 6. Immune cells in the brain of MPTPp mice treated with ECS modulators. MPTPp mice were treated with JWH133, RO304, JZL184 or vehicle for 5 weeks. After sacrifice, the striatum and the ventral midbrain were dissected to prepare cell suspensions for flow cytometry analysis. Relative amounts of (A) $CD4^+$, (B) $CD8^+$, (C) $CD11b^+CD45^{low}$ and (D) $CD11b^+CD45^{high}$ cell subsets. The effect of compounds, JZL184, JWH133 and RO304 on T cell activation was determined as the percentage of $TNF\alpha^+$ in (E) $CD4^+$ and in $CD8^+$ T cells in the ventral midbrain. The dashed line corresponds to the mean value in control animals. Data represent the mean ± 95 % CI of 4–9 animals/group. Statistical analysis: One-way ANOVA followed by Bonferroni's multiple comparison test for data with normal distribution. Kruskal-Wallis followed by Dunn's multiple comparison test for data not following a normal distribution, $*p < 0.05$, $**p < 0.01$, $***p < 0.001$.

CXCL12-induced T-cell chemotaxis at the peak of CB2R expression induced by 2-AG and JWH133 (Coopman et al., 2007). Taken together, these data suggest that the presence of $CD4^+$ cells exerts detrimental effects on dopaminergic neurons in chronic stages.

The anti-inflammatory properties of CB2R agonists make them a promising pharmacological alternative to counteract inflammatory response in multiple sclerosis and stroke (Tiberi et al., 2022; Maresz et al., 2007; Zarruk et al., 2012). In experimental models of Alzheimer's disease, mice lacking CB2R show a reduced proinflammatory response without impairing memory and learning (Reusch et al., 2022). In contrast, neuroinflammation induced by graft-*vs*-host disease is ameliorated by CB2R inverse agonist/antagonists and CB2R deletion (Moe et al., 2024). In the latter inflammatory context, the general functions of CB2Rs are to promote leukocyte recruitment into the brain and to regulate the balance between TNFα and IFNγ (Moe et al., 2024). In the MPTPp mouse model, we achieve neuroprotection by the same mechanisms proposed by Moe et al. (2024), reduced $CD4^+$ T cell recruitment and TNFα production, which are induced by CB2R activation and abolished in CB2R KO mice. We also show that host activation of CB2R in the brain of chimeric mice is required for neuroprotection. The increase in 2-AG by JZL184 may induce an activation of CB1R in neurons or in astrocytes. However, we have shown in this study that the neuroprotective effect of the drug and its modulatory effect on the immune response depend on CB2R activation. Chimeric host mice lacking CB2R were highly sensitive to MPTPp and most animals did not reach the endpoint of the experiment. A similar observation has been reported for acute MPTP administration to CB2R-deficient mice (Price et al., 2009). These results suggest that CB2R expression in the brain, mainly in microglia, counteracts the effects of neuronal death by MPTP administration. As we have previously reported, the effect of MAGL inhibition on neuronal survival is mediated by CB2R and depends on the presence of glial cells (Rojo-Bustamante et al., 2020). In addition, our group has shown that the basal inflammatory tone of the midbrain is different from other brain regions and, consequently, the inflammatory response elicited by lipopolysaccharide (LPS) is region dependent (Abellanas et al., 2019). The different transcriptomic profile between striatal and midbrain myeloid cells (Abellanas et al., 2019) may trigger alternative inflammatory pathways upon CB2R activation. In the time course of MPTPp-induced dopaminergic degeneration, the progressive increase in CB2R expression parallels the acquisition of a phagocytic and proinflammatory profile in microglia (Ayerra et al., 2024). CB2R is not required for the generation of LPS/IFNγ-induced microglial activation (Olabiyi et al., 2023), but it is involved in the acquisition of an alternative and phagocytic phenotype (Mecha et al., 2015). In the MPTPp mouse model, CB2R activation by elevated 2-AG levels may polarize toward a neuroprotective phenotype.

The enzymatic hydrolysis of 2-AG is primarily mediated by MAGL, which is the major regulator of 2-AG levels in the brain (Nomura et al., 1979; Viader et al., 2015). Microglia express the components required for eCB autocrine or paracrine signaling (Stella, 2009). In the midbrain from human PD patients, downregulation of 2-AG synthesizing enzymes (*DAGLB*, *PLCB2* and *PLD1*) and upregulation of 2-AG degrading enzyme *(ABDHD3)* suggest a reduced production of this endocannabinoid by microglia. The transcriptomic profile in the same cells (Smajic et al., 2022) predicts an upregulation of the *Th1 pathway, IFNγ signaling* and *T cell infiltration* (Ayerra et al., 2024). Upregulation of IFNγ signaling in the human midbrain may interfere with 2-AG production and neuroprotection (Witting et al., 2006). The increased CB2R receptor

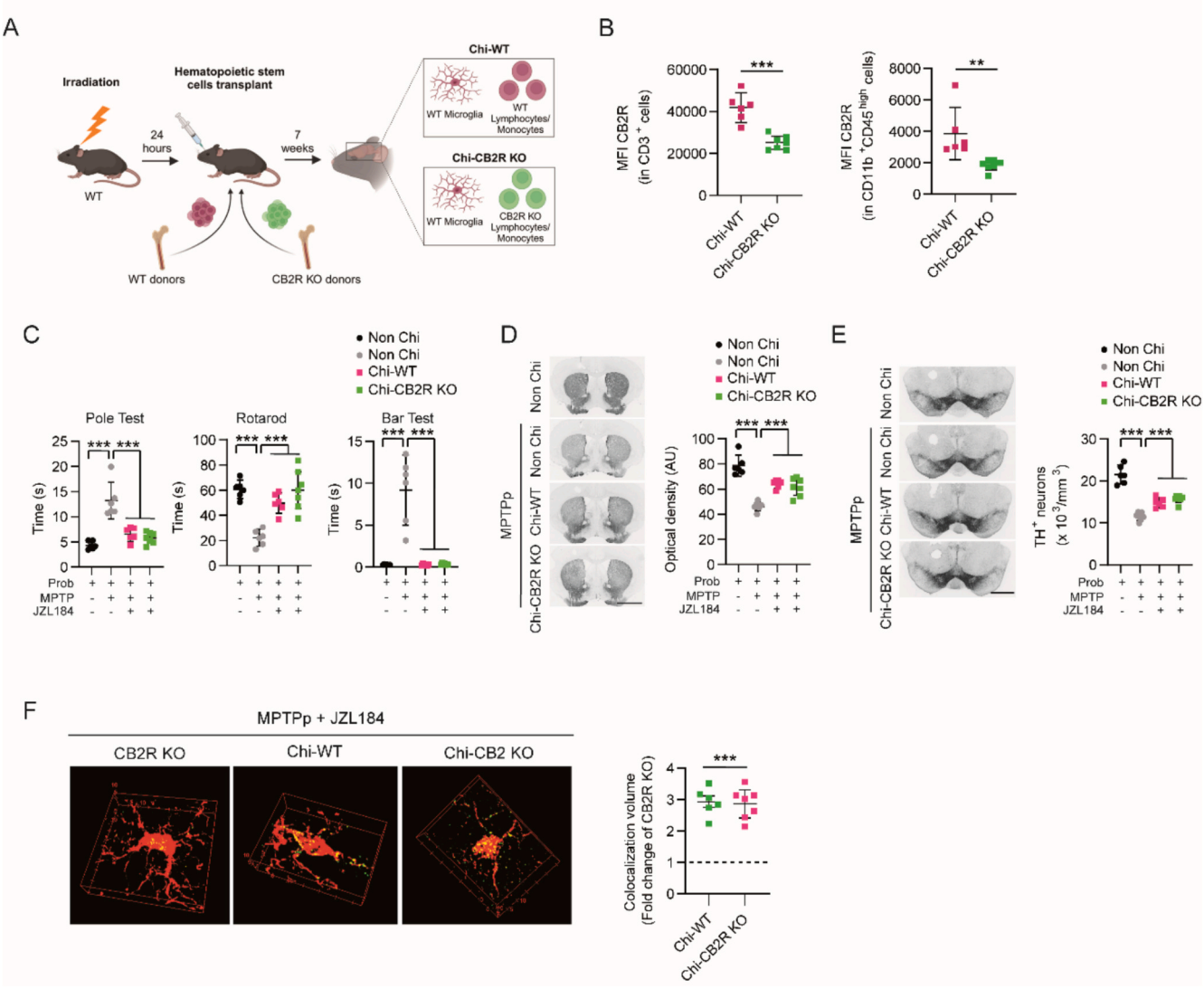

Fig. 7. Analysis of the neuroprotective effect of JZL184 in MPTP-intoxicated chimeric mice. (A) Scheme showing the generation of bone marrow chimeric mice. WT mice were transplanted with HSCs from WT (Chi-WT) or CB2R KO (Chi-CB2R KO) mice 24 h after irradiation and allowed to recover for 7 weeks. (B) CB2R expression in $CD3^+$ and $CD11b^+CD45^{high}$ cells from submandibular blood samples. Chronic JZL184 treatment was evaluated in the chimeric mice after the induction of the MPTPp model: (C) motor behavior was evaluated in the pole, rotarod, and bar tests; (D) representative images showing TH immunoreactivity and optical density analysis of the TH signal in the striatum; (E) representative images showing TH^+ dopaminergic neurons and stereological quantification of the number of TH^+ neurons in the SNpc. (F) Representative 3D reconstructions of Iba1/CB2R double immunofluorescence in the SNpc of CB2R KO mice as negative control and Chi-WT and Chi-CB2R KO mice and the corresponding quantification of Iba1-CB2R colocalization volume. Data represent the mean ± 95 % CI from 6 to 7 animals/group. Statistical analysis: (B and F) *t*-test for data following a normal distribution with Welch correction for significantly different variances. Mann-Whitney test for data not following a normal distribution. (C-E) One-way ANOVA followed by Bonferroni's multiple comparison test for data following a normal distribution. Kruskal-Wallis followed by Dunn's multiple comparison test for data not following a normal distribution, $^{**}p < 0.01$, $^{***}p < 0.001$. Magnification bars: (D) 2 mm, (E) 1 mm, (F) 5 and 10 μm.

expression observed in microglial cells in the SNpc of PD patients (Gómez-Gálvez et al., 2016) is reproduced in the experimental MPTPp mouse model. Taken together, these data support the potential benefits of MAGL inhibition to increase 2-AG levels in the context of dopaminergic degeneration. Several studies have described an increased Th1 response in peripheral $CD4^+$ T cells in PD patients, suggesting a potential entry of lymphocytes across the BBB. The reduction in TNFα production by $CD4^+$ and $CD8^+$ T cells may contribute to the neuroprotective effect. These findings are consistent with the reduced incidence of PD in patients treated with anti-TNFα therapy (Peter et al., 2018).

Our results demonstrate that the neuroprotective effect of JZL184 in the MPTPp mouse model of PD is mediated by CB2R. The BBB-permeable CB2R agonist (JWH133) reproduced the effect of JZL184, whereas the peripheral CB2R agonist (RO304) failed to ameliorate the parkinsonian condition. CB2R activation in the brain is required for neuroprotection and prevention of CD4 T cell recruitment to the midbrain and T cell production of TNFα. The expression of the ECS elements in midbrain microglia of PD patients supports the potential therapeutic benefit of MAGL inhibition or central CB2R activation for the treatment of PD.

CRediT authorship contribution statement

Leyre Ayerra: Writing – original draft, Methodology, Investigation, Funding acquisition. **Miguel Angel Abellanas:** Writing – review & editing, Methodology, Investigation, Data curation, Conceptualization. **Clara Vidaurre:** Writing – review & editing, Methodology,

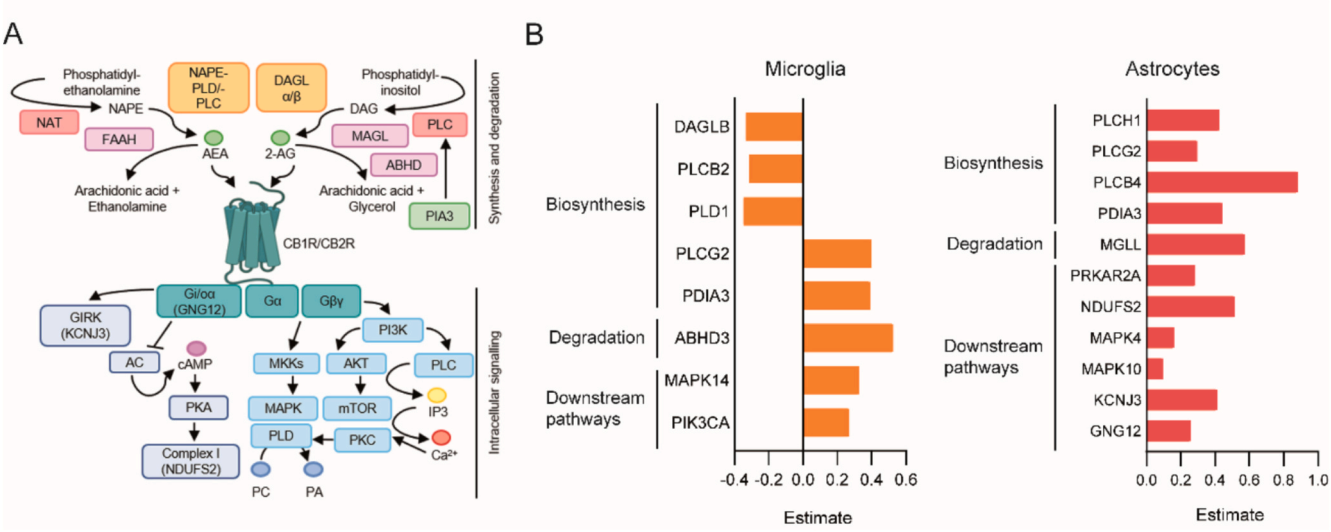

Fig. 8. Differentially expressed ECS transcripts from human PD midbrain. ECS transcripts related to 2-AG metabolism were extracted from differentially expressed gene sets from the midbrain of IPD. (A) Schematic representation of synthesis and degradation-related pathways and intracellular signaling cascades related to the ECS. Upregulated (estimate > 0) and downregulated (estimate < 0) differentially expressed genes ($q < 0.05$) from microglia (A) and astrocytes (B) in the human PD midbrain.

Investigation. **Leyre Basurco:** Writing – review & editing, Methodology, Investigation, Data curation. **Adriana Tavira:** Writing – review & editing, Methodology, Investigation. **Esther Luquin:** Writing – review & editing, Supervision, Methodology, Investigation, Formal analysis. **Pedro Clavero:** Writing – review & editing, Supervision, Conceptualization. **Elisa Mengual:** Writing – review & editing, Supervision. **Maria Collantes:** Writing – review & editing, Methodology, Investigation. **Ivan Peñuelas:** Writing – review & editing, Supervision, Conceptualization. **Samuel Ruiz de Martin-Esteban:** Writing – review & editing, Methodology. **Uwe Grether:** Writing – review & editing, Resources, Methodology, Conceptualization. **Cecilia J. Hillard:** Writing – review & editing, Resources, Conceptualization. **Julian Romero:** Writing – review & editing, Resources, Conceptualization. **Sandra Hervás-Stubbs:** Writing – review & editing, Supervision, Methodology, Investigation, Conceptualization. **Maria S. Aymerich:** Writing – original draft, Supervision, Resources, Project administration, Methodology, Investigation, Formal analysis, Conceptualization.

Funding

This work was supported by the Spanish Government Instituto de Salud Carlos III, ISCIII-FEDER PI20/01063, Ministerio de Ciencia e Innovación MCIN/AEI/FEDER PID2022-138461OB-I00 and Fundación Gangoiti. LA was funded by FPU19/03255; LB was funded by FPU018/02244; AT was funded by FPU21/01545.

Declaration of competing interest

The authors declare the following financial interests/personal relationships which may be considered as potential competing interests: CJH is a scientific advisor and has equity in Formulate Biosciences, Inc. UG is a full employee of F. Hoffmann-La Roche Ltd.

Acknowledgements

We acknowledge the support of Diego Alignani from the flow cytometry facility for his guidance with the FACS analysis. We acknowledge the technical support of Beatriz Paternain and Amaya Trigo.

Appendix A. Supplementary data

Supplementary data to this article can be found online at https://doi.org/10.1016/j.bbi.2025.04.037.

Data availability

Data will be made available on request.

References

Freund, T.F., Katona, I., Piomelli, D., 2003. Role of endogenous cannabinoids in synaptic signaling. Physiol. Rev. 83 (3), 1017–1066.
Salzet, M., Breton, C., Bisogno, T., Di Marzo, V., 2000. Comparative biology of the endocannabinoid system possible role in the immune response. Eur. J. Biochem. 267 (16), 4917–4927.
Aymerich, M.S., Aso, E., Abellanas, M.A., Tolon, R.M., Ramos, J.A., Ferrer, I., et al., 2018. Cannabinoid pharmacology/therapeutics in chronic degenerative disorders affecting the central nervous system. Biochem. Pharmacol. 157, 67–84.
Munro, S., Thomas, K.L., Abu-Shaar, M., 1993. Molecular characterization of a peripheral receptor for cannabinoids. Nature 365 (6441), 61–65.
Galiègue, S., Mary, S., Marchand, J., Dussossoy, D., Carrière, D., Carayon, P., et al., 1995. Expression of central and peripheral cannabinoid receptors in human immune tissues and leukocyte subpopulations. Eur. J. Biochem. 232 (1), 54–61.
Núñez, E., Benito, C., Pazos, M.R., Barbachano, A., Fajardo, O., González, S., et al., 2004. Cannabinoid CB2 receptors are expressed by perivascular microglial cells in the human brain: an immunohistochemical study. Synapse 53 (4), 208–213.
Brusco, A., Tagliaferro, P., Saez, T., Onaivi, E.S., 2008. Postsynaptic localization of CB2 cannabinoid receptors in the rat hippocampus. Synapse 62 (12), 944–949.
Benito, C., Núñez, E., Tolón, R.M., Carrier, E.J., Rábano, A., Hillard, C.J., et al., 2003. Cannabinoid CB 2 receptors and fatty acid amide hydrolase are selectively overexpressed in neuritic plaque-associated glia in Alzheimer's disease brains. J. Neurosci. 23 (35), 11136–11141.
Benito, C., Romero, J.P., Tolón, R.M., Clemente, D., Docagne, F., Hillard, C.J., et al., 2007. Cannabinoid CB1 and CB2 receptors and fatty acid amide hydrolase are specific markers of plaque cell subtypes in human multiple sclerosis. J. Neurosci. 27 (9), 2396–2402.
Gómez-Gálvez, Y., Palomo-Garo, C., Fernández-Ruiz, J., García, C., 2016. Potential of the cannabinoid CB(2) receptor as a pharmacological target against inflammation in Parkinson's disease. Prog. Neuropsychopharmacol. Biol. Psychiatry 4 (64), 200–208.
Tansey, M.G., Wallings, R.L., Houser, M.C., Herrick, M.K., Keating, C.E., Joers, V., 2022. Inflammation and immune dysfunction in Parkinson disease. Nat. Rev. Immunol. 22 (11), 657–673.
Pierce, S., Coetzee, G.A., 2017. Parkinson's disease-associated genetic variation is linked to quantitative expression of inflammatory genes. PLoS One.
Nalls, M.A., Blauwendraat, C., Vallerga, C.L., Heilbron, K., Bandres-Ciga, S., Chang, D., et al., 2019. Identification of novel risk loci, causal insights, and heritable risk for Parkinson's disease: a meta-analysis of genome-wide association studies. Lancet Neurol. 18 (12), 1091–1102.

Witoelar, A., Jansen, I.E., Wang, Y., Desikan, R.S., Gibbs, J.R., Blauwendraat, C., et al., 2017. Genome-wide pleiotropy between Parkinson disease and autoimmune diseases. JAMA Neurol. 74 (7), 780–792.
Hui, K.Y., Fernandez-Hernandez, H., Hu, J., Schaffner, A., Pankratz, N., Hsu, N.Y., et al., 2018. Functional variants in the LRRK2 gene confer shared effects on risk for Crohn's disease and Parkinson's disease. Sci. Transl. Med.
Harms, A.S., Yang, Y.T., Tansey, M.G., 2023. Central and peripheral innate and adaptive immunity in Parkinson's disease. Sci. Transl. Med.
McGeer, P.L., Itagaki, S., Boyes, B.E., McGeer, E.G., 1988. Reactive microglia are positive for HLA-DR in the substantia nigra of Parkinson's and Alzheimer's disease brains. Neurology 38 (8), 1285–1291.
Imamura, K., Hishikawa, N., Sawada, M., Nagatsu, T., Yoshida, M., Hashizume, Y., 2003. Distribution of major histocompatibility complex class II-positive microglia and cytokine profile of Parkinson's disease brains. Acta Neuropathol. 106 (6), 518–526.
Hunot, S., Dugas, N., Faucheux, B., Hartmann, A., Tardieu, M., Debré, P., et al., 1999. FcεRII/CD23 is expressed in Parkinson's disease and induces, in vitro, production of nitric oxide and tumor necrosis factor-α in glial cells. J. Neurosci. 19 (9), 3440–3447.
Harms, A.S., Delic, V., Thome, A.D., Bryant, N., Liu, Z., Chandra, S., et al., 2017 21. α-Synuclein fibrils recruit peripheral immune cells in the rat brain prior to neurodegeneration. Acta Neuropathol. Commun. 5 (1), 85.
Ayerra, L., Abellanas, M.A., Basurco, L., Tamayo, I., Conde, E., Tavira, A., et al., 2024. Nigrostriatal degeneration determines dynamics of glial inflammatory and phagocytic activity. J. Neuroinflammation 21 (1), 92.
Brochard, V., Combadière, B., Prigent, A., Laouar, Y., Perrin, A., Beray-Berthat, V., et al., 2009. Infiltration of CD4+ lymphocytes into the brain contributes to neurodegeneration in a mouse model of Parkinson disease. J. Clin. Invest. 119 (1), 182–192.
Galiano-Landeira, J., Torra, A., Vila, M., Bové, J., 2020. CD8 T cell nigral infiltration precedes synucleinopathy in early stages of Parkinson's disease. Brain [internet]. 143 (12), 3717–3733.
Grozdanov, V., Bliederhaeuser, C., Ruf, W.P., Roth, V., Fundel-Clemens, K., Zondler, L., et al., 2014. Inflammatory dysregulation of blood monocytes in Parkinson's disease patients. Acta Neuropathol. 2014;128(5):651–63.
Funk, N., Wieghofer, P., Grimm, S., Schaefer, R., Bühring, H.J., Gasser, T., et al., 2013. Characterization of peripheral hematopoietic stem cells and monocytes in Parkinson's disease. Mov. Disord. 28 (3), 392–395.
Schlachetzki, J.C.M., Prots, I., Tao, J., Chun, H.B., Saijo, K., Gosselin, D., et al., 2018. A monocyte gene expression signature in the early clinical course of Parkinson's disease. Sci. Rep. 8 (1), 10757.
Pike, S.C., Havrda, M., Gilli, F., Zhang, Z., Salas, L.A., 2024. Immunological shifts during early-stage Parkinson's disease identified with DNA methylation data on longitudinally collected blood samples. NPJ Parkinsons Dis. 10 (1), 21.
Mamula, D., Khosousi, S., He, Y., Lazarevic, V., Svenningsson, P., 2022. Impaired migratory phenotype of CD4+ T cells in Parkinson's disease. NPJ Parkinsons Dis. 8 (1), 171.
Celorrio, M., Fernández-Suárez, D., Rojo-Bustamante, E., Echeverry-Alzate, V., Ramírez, M.J., Hillard, C.J., et al., 2016. Fatty acid amide hydrolase inhibition for the symptomatic relief of Parkinson's disease. Brain Behav. Immun. 57, 94–105.
Fernández-Suárez, D., Celorrio, M., Riezu-Boj, J.I., Ugarte, A., Pacheco, R., González, H., et al., 2014. The monoacylglycerol lipase inhibitor JZL184 is neuroprotective and alters glial cell phenotype in the chronic MPTP mouse model. Neurobiol. Aging 35 (11), 2603–2616.
Celorrio, M., Rojo-Bustamante, E., Fernández-Suárez, D., Sáez, E., Estella-Hermoso de Mendoza, A., Müller, C.E., et al., 2017. GPR55: a therapeutic target for Parkinson's disease? Neuropharmacology 125, 319–332.
Blankman, J.L., Simon, G.M., Cravatt, B.F., 2007. A comprehensive profile of brain enzymes that hydrolyze the endocannabinoid 2-arachidonoylglycerol. Chem. Biol. 14 (12), 1347–1356.
Mecha, M., Feliú, A., Machín, I., Cordero, C., Carrillo-Salinas, F., Mestre, L., et al., 2018. 2-AG limits Theiler's virus induced acute neuroinflammation by modulating microglia and promoting MDSCs. Glia 66 (7), 1447–1463.
Gonsiorek, W., Lunn, C., Fan, X., Narula, S., Lundell, D., Hipkin, R.W., 2000. Endocannabinoid 2-arachidonyl glycerol is a full agonist through human type 2 cannabinoid receptor: antagonism by anandamide. Mol. Pharmacol. 57 (5), 1045–1050.
Nomura, D.K., Morrison, B.E., Blankman, J.L., Long, J.Z., Kinsey, S.G., Marcondes, M.C., et al., 1979. Endocannabinoid hydrolysis generates brain prostaglandins that promote neuroinflammation. Science 334 (6057), 809–813.
Aymerich, M.S., Rojo-Bustamante, E., Molina, C., Celorrio, M., Sánchez-Arias, J.A., Franco, R., 2016. Neuroprotective effect of JZL184 in MPP(+)-treated SH-SY5Y cells through CB2 receptors. Mol. Neurobiol. 53 (4), 2312–2319.
Xu, K., Xu, Y., Brown-Jermyn, D., Chen, J.F., Ascherio, A., Dluzen, D.E., et al., 2006. Estrogen prevents neuroprotection by caffeine in the mouse 1-methyl-4-phenyl-1,2,3,6-tetrahydropyridine model of Parkinson's disease. J. Neurosci. 26 (2), 535–541.
Miller, D.B., Ali, S.F., O'Callaghan, J.P., Laws, S.C., 1998. The impact of gender and estrogen on striatal dopaminergic neurotoxicity. Ann. N. Y. Acad. Sci. 30 (844), 153–165.
López, A., Aparicio, N., Pazos, M.R., Grande, M.T., Barreda-Manso, M.A., Benito-Cuesta, I., et al., 2018. Cannabinoid CB2 receptors in the mouse brain: relevance for Alzheimer's disease. J. Neuroinflammation 15 (1), 158.
Martín-Moreno, A.M., Brera, B., Spuch, C., Carro, E., García-García, L., Delgado, M., et al., 2012. Prolonged oral cannabinoid administration prevents neuroinflammation, lowers β-amyloid levels and improves cognitive performance in Tg APP 2576 mice. J. Neuroinflammation 16 (9), 8.
Aso, E., Juvés, S., Maldonado, R., Ferrer, I., 2013. CB2 cannabinoid receptor agonist ameliorates Alzheimer-like phenotype in AβPP/PS1 mice. J. Alzheimers Dis. 35 (4), 847–858.
Nettekoven, M., Adam, J.M., Bendels, S., Bissantz, C., Fingerle, J., Grether, U., et al., 2016. Novel triazolopyrimidine-derived cannabinoid receptor 2 agonists as potential treatment for inflammatory kidney diseases. ChemMedChem 11 (2), 179–189.
Gundersen, H.J., Jensen, E.B., 1987. The efficiency of systematic sampling in stereology and its prediction. J. Microsc. 147 (Pt 3), 229–263.
Smajic, S., Prada-Medina, C.A., Landoulsi, Z., Ghelfi, J., Delcambre, S., Dietrich, C., et al., 2022. Single-cell sequencing of human midbrain reveals glial activation and a Parkinson-specific neuronal state. Brain 145 (3), 964–978.
Gómez-Gálvez, Y., Palomo-Garo, C., 2016. Potential of the cannabinoid CB 2 receptor as a pharmacological target against inflammation in Parkinson's disease. Prog. Neuropsychopharmacol. Biol. Psychiatry 64, 200–208.
Mecha, M., Feliú, A., Carrillo-Salinas, F.J., Rueda-Zubiaurre, A., Ortega-Gutiérrez, S., de Sola, R.G., et al., 2015. Endocannabinoids drive the acquisition of an alternative phenotype in microglia. Brain Behav. Immun. 49, 233–245.
Reusch, N., Ravichandran, K.A., Olabiyi, B.F., Komorowska-Müller, J.A., Hansen, J.N., Ulas, T., et al., 2022. Cannabinoid receptor 2 is necessary to induce toll-like receptor-mediated microglial activation. Glia 70 (1), 71–88.
Soethoudt, M., Grether, U., Fingerle, J., Grim, T.W., Fezza, F., de Petrocellis, L., et al., 2017. Cannabinoid CB2 receptor ligand profiling reveals biased signalling and off-target activity. Nat. Commun. 3 (8), 13958.
Porter, R.F., Szczesniak, A.M., Toguri, J.T., Gebremeskel, S., Johnston, B., Lehmann, C., et al., 2019. Selective cannabinoid 2 receptor agonists as potential therapeutic drugs for the treatment of endotoxin-induced uveitis. Molecules.
Mildner, A., Schmidt, H., Nitsche, M., Merkler, D., Hanisch, U.K., Mack, M., et al., 2007. Microglia in the adult brain arise from Ly-6ChiCCR2+ monocytes only under defined host conditions. Nat. Neurosci. 10 (12), 1544–1553.
Harms, A.S., Cao, S., Rowse, A.L., Thome, A.D., Li, X., Mangieri, L.R., et al., 2013. MHCII is required for α-synuclein-induced activation of microglia, CD4 T cell proliferation, and dopaminergic neurodegeneration. J. Neurosci. 33 (23), 9592–9600.
Basurco, L., Abellanas, M.A., Ayerra, L., Conde, E., Vinueza-Gavilanes, R., Luquin, E., et al., 2023. Microglia and astrocyte activation is region-dependent in the α-synuclein mouse model of Parkinson's disease. Glia 71 (3), 571–587.
Coopman, K., Smith, L.D., Wright, K.L., Ward, S.G., 2007. Temporal variation in CB2R levels following T lymphocyte activation: evidence that cannabinoids modulate CXCL12-induced chemotaxis. Int. Immunopharmacol. 7 (3), 360–371.
Tiberi, M., Evron, T., Saracini, S., Boffa, L., Mercuri, N.B., Chintalacharuvu, S.R., et al., 2022. Potent T cell-mediated anti-inflammatory role of the selective CB2 agonist lenabasum in multiple sclerosis. Neuropathol. Appl. Neurobiol.
Maresz, K., Pryce, G., Ponomarev, E.D., Marsicano, G., Croxford, J.L., Shriver, L.P., et al., 2007. Direct suppression of CNS autoimmune inflammation via the cannabinoid receptor CB1 on neurons and CB2 on autoreactive T cells. Nat. Med. 13 (4), 492–497.
Zarruk, J.G., Fernández-López, D., García-Yébenes, I., García-Gutiérrez, M.S., Vivancos, J., Nombela, F., et al., 2012. Cannabinoid type 2 receptor activation downregulates stroke-induced classic and alternative brain macrophage/microglial activation concomitant to neuroprotection. Stroke 43 (1), 211–219.
Moe, A., Rayasam, A., Sauber, G., Shah, R.K., Doherty, A., Yuan, C.Y., et al., 2024. Type 2 cannabinoid receptor expression on microglial cells regulates neuroinflammation during graft-versus-host disease. J. Clin. Invest.
Price, D.A., Martinez, A.A., Seillier, A., Koek, W., Acosta, Y., Fernandez, E., et al., 2009. WIN55,212-2, a cannabinoid receptor agonist, protects against nigrostriatal cell loss in the 1-methyl-4-phenyl-1,2,3,6-tetrahydropyridine mouse model of Parkinson's disease. Eur. J. Neurosci. 29 (11), 2177–2186.
Rojo-Bustamante, E., Íñigo-Marco, I., Abellanas, M.A., Vinueza-Gavilanes, R., Baltanás, A., Luquin, E., et al., 2020. CB2 receptors and neuron-glia interactions modulate neurotoxicity generated by MAGL inhibition. Biomolecules.
Abellanas, M.A., Zamarbide, M., Basurco, L., Luquin, E., Garcia-Granero, M., Clavero, P., et al., 2019. Midbrain microglia mediate a specific immunosuppressive response under inflammatory conditions. J. Neuroinflammation 16 (1), 233.
Olabiyi, B.F., Schmoele, A.C., Beins, E.C., Zimmer, A., 2023. Pharmacological blockade of cannabinoid receptor 2 signaling does not affect LPS/IFN-γ-induced microglial activation. Sci. Rep. 13 (1), 11105.
Viader, A., Blankman, J.L., Zhong, P., Liu, X., Schlosburg, J.E., Joslyn, C.M., et al., 2015. Metabolic interplay between astrocytes and neurons regulates endocannabinoid action. Cell Rep. 12 (5), 798–808.
Stella, N., 2009. Endocannabinoid signaling in microglial cells. Neuropharmacology 56 (Suppl 1), 244–253.
Witting, A., Chen, L., Cudaback, E., Straiker, A., Walter, L., Rickman, B., et al., 2006. Experimental autoimmune encephalomyelitis disrupts endocannabinoid-mediated neuroprotection. PNAS 103 (16), 6362–6367.
Peter, I., Dubinsky, M., Bressman, S., Park, A., Lu, C., Chen, N., et al., 2018. Anti-tumor necrosis factor therapy and incidence of parkinson disease among patients with inflammatory bowel disease. JAMA Neurol. 75 (8), 939–946.